Prediction of size distribution in dairy cream homogenization

Olivier Masbernat, Frédéric Risso, Benjamin Lalanne, Simon Bugeat, Mikaël Berton

Graphical Abstract

Prediction of size distribution in dairy cream homogenization

Olivier Masbernat,Frédéric Risso,Benjamin Lalanne,Simon Bugeat,Mikaël Berton

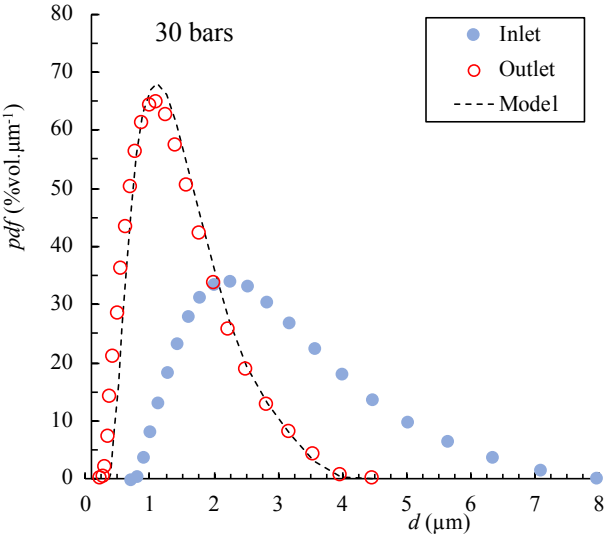

Highlights

Prediction of size distribution in dairy cream homogenization

Olivier Masbernat,Frédéric Risso,Benjamin Lalanne,Simon Bugeat,Mikaël Berton

- Homogenized fat globules size distribution in cream can be deduced from the entry size distribution with a single parameter.
- A simple viscous shear dominated breakup model is proposed to interpret this result.
- The breakup model parameter can be explicitely related to the *HPH* pressure.

Prediction of size distribution in dairy cream homogenization

Olivier Masbernat[a,c,*], Frédéric Risso[b,c], Benjamin Lalanne[a,c], Simon Bugeat[d] and Mikaël Berton[e,1]

[a] *Laboratoire de Génie Chimique, Université de Toulouse, CNRS, BP 84234, 4 allée Emile Monso, 31432 Toulouse, France*
[b] *Institut de Mécanique des Fluides de Toulouse, Université de Toulouse, CNRS, 2 Allée du Professeur Camille Soula,31400 Toulouse, France*
[c] *Fédération de Recherche FERMAT, Université de Toulouse, CNRS, Toulouse, France*
[d] *SODIAAL International, 1-3 rue Jules Maillard de la Gournerie, ZAC Atalante Champeau, 35000 Rennes, France*
[e] *Lemma Engineering, 1110 avenue de l'Occitanie, Technoparc 1, Bât. 4, 31670 Labège, France*

ARTICLE INFO

Keywords:
High-pressure homogenizer
cream fat globules
Breakup
Size distribution

ABSTRACT

The size distribution of fat globules in homogenized concentrated dairy cream has been measured in High-Pressure Homogenizers (*HPH*), working at 80°C and various operating pressures. For each pressure, the outlet size distribution is found to be self-similar to the inlet distribution, and can be accurately predicted dividing each class diameter of the inlet distribution by a single proportionality factor, which can be interpreted using a simplified deformation model of the fat globules as elongated filaments. The evolution of the factor with the operating pressure is consistent with a scaling analysis of the dissipation rate in the *HPH* as well as with the value predicted from numerical simulations of the flow in the *HPH*, supporting the physical interpretation of the fragmentation model.

1. Introduction

Homogenization of emulsions consists in reducing the average size of micrometer-size droplets down to the order of a few hundred nanometers and is commonly performed in dairy industry for more than a century (**???**). The knowledge of size distribution and composition of the interface of fat globules after homogenization is crucial regarding a number of issues, such as metastability (**?**), rheology and texture of the resulting suspension (**??**). High-Pressure Homogenizer (*HPH*) is an apparatus in which the emulsion is forced to flow at a (nearly) constant flowrate within a thin gap where it is highly accelerated, before merging in an outlet chamber or impact ring where it is highly sheared. The high mean shear rates and induced turbulence produced in the chamber are responsible for the deformation and breakup of the emulsion droplets. Therefore, predicting the size distribution in such a flow geometry *a priori* requires to model the fragmentation statistics in a complex highly heterogeneous turbulent flow with very short residence times (**???**). In the case of concentrated emulsions with complex interfaces such as a dairy cream, this problem is even more complicated due to additional bulk and interfacial rheology issues (**??**). In particular, it is likely that classical Hinze-Kolmogorov theory which is often applied to model the breakup process of a drop in turbulent flows (**?**) is not

*Corresponding author
olivier.masbernat@ensiacet.fr (O. Masbernat); frisso@imft.fr (F. Risso); benjamin.lalanne@ensiacet.fr (B. Lalanne); Simon.BUGEAT@Sodiaal.fr (S. Bugeat); m.berton@absolutcooking.com (M. Berton)
https://www.lemma-ing.com (M. Berton)
ORCID(s):
[1] Present address: Absolut Cooking, 25 ter route de Caussidières 31560 Nailloux, France

appropriate in the case of high-viscosity milk fat globules, which can be stretched over length scales that may exceed any of the turbulent length scale present in the flow. For such systems, it seems that only macroscopic correlations relating mean or maximum stable diameter to the dissipation rate or operating pressure in the *HPH* can be proposed to the food processing engineers (**?**). Such correlations are of limited range regarding the upscaling issue of homogenization processes. In the present work, the size distributions of the fat globules resulting from the homogenization of dairy cream at various (moderate) pressures have been measured in two *HPHs*: a pilot one at a reduced scale, and an industrial one at practical operating conditions. The comparison of measured outlet size distributions with those of native fat globules before homogenization revealed a simple breakup mechanism that that can be modeled by considering the viscous deformation of a droplet under an unsteady shear flow, in the absence of any shape relaxation. This simple model provides an accurate prediction of the size distribution of fat globules in homogenized dairy cream.

2. Materials and methods

2.1. Cream properties

Raw milk is collected from farms in the area of St Etienne (France) and stored at 4°C. The cream is produced at a flowrate of 20×10^3 L/h from a centrifugal plate skimmer (Westfalia Separator Type MSA 160-01-076) operated at 4700 rpm. The fat content of the cream, measured by infrared spectroscopy (Delta Instruments, Lactoscope FTIR FTA-3.4), is close to 400 g/L. Then it is adjusted to 35% w/w by addition of skimmed milk to the cream. The cream is then stored at 4°C during 2 to 4 hours. A sample of the cream is collected for granulometric analysis. A sample of butter (82% fat) was melted at 80°C in a falcon tube during 10 minutes and the fat was collected after water demixing. The internal viscosity of the fat globules was measured on milk fat samples extracted at 80°C from melted butter produced in the site of SODIAAL in Clermont-Ferrand during the same period the cream was produced, with no significant difference in fatty acids composition between cream and butter. Rheological properties of the fat extracted from the butter and the cream are therefore similar. The viscosity of fat was determined from stress-shear rate curves measured at controlled temperatures (75, 80 and 85°C) in a cone/plate viscometer (Brookfield DV-I Prime, BE, UK). Measurements were performed with a shear rate ranging between 2 and 40 s^{-1}. A slight shear-shinning behavior is observed in the lower range of shear rate, followed by a Newtonian plateau above 10 s^{-1}. The fat viscosity measured at 80°C is 10.5×10^{-3}. The cream density ρ_e and viscosity μ_e at 80°C can be estimated respectively to 960 kg/m^3 and 2.9×10^{-3}, from the correlations proposed by **?**.

2.2. Size distribution measurement

Cream samples are prepared as follows: 1 mL of homogenized cream is diluted in 9 mL of an aqueous solution containing 1% w/w of Sodium Dodecyl Sulfate (SDS) and 35 mM of Ethylene-diamine-tetra-acetic acid (EDTA), adjusted at pH=7 at ambient temperature. SDS prevents the flocculation of fat globules and EDTA dissociates casein micelles and prevents the appearance of a parasite peak around 100 nm in the size distribution (**?**). Few drops of this solution are introduced in the measurement cell of a Static Light Scattering granulometer (Mastersizer 2000, Malvern Instruments, UK). The light sources are a He/Ne laser at 633 nm and a electroluminescent diode at 466 nm. Refractive indices selected for the measurements are 1.33 for the dispersing medium (water), and 1.452 and 1.460 for the milk fat, at respectively 633 and 466 nm, as prescribed by **?**. Measurements were performed with an obscuration rate of 2% after the measurement of the noise level in water. The size distributions in volume were averaged over 3 consecutive measurements.

2.3. *HPH* equipment

Two High Pressure Homogenizers (*HPHs*) of different brands were used in this study, one at pilot scale and one at industrial scale. The pilot HPH is a GEA Niro Soavi NS3015H, and the industrial *HPH* is a TETRAPAK Alex Homogenizer 400. The flowrate Q was 200 L/h in the pilot and 8800 L/h in industrial scale *HPHs*, which corresponds to the same residence time T_r (ratio between the *HPH* volume and the flowrate) of the emulsion in both *HPHs* (T_r=0.09 s). The typical internal geometry of a *HPH* is schematized in Fig. 1. It's an axially symmetric valve composed of an inlet section of radius R_0 (of a few millimeters) through which the dairy emulsion is injected by a volumetric pump at a flowrate $Q = \pi R_0^2 U_0$ and is then forced to flow through a narrow gap of thickness δ, which is two orders of magnitude smaller than R_0.The emulsion is highly accelerated in the gap up to a velocity U_δ forming a jet that rams the wall of the impact ring, before flowing out of the device. More on the internal geometry of the two *HPHs* is given in appendix B. With this geometry, mass conservation imposes that $U_\delta = U_0 R_0/(2\delta)$, so $U_\delta >> U_0$. A simplified Bernouilli equation therefore gives an estimate of the pressure drop ΔP in a *HPH* as $\Delta P \sim \rho_e U_\delta^2$ (with ρ_e the emulsion density). For a typical pressure of 100 bars in a *HPH*, the emulsion reaches a velocity U_δ of the order of 100 m/s. The break-up of the emulsion drops occurs in the impact ring chamber (of width $L_R \sim O(10^2 \times \delta)$) where the shear rate produced is intense ($U_\delta / L_R \sim 10^5\ s^{-1}$). In this study, the operating pressure ΔP used for the concentrated dairy cream homogenization ranges between 15 and 60 bars in the pilot *HPH* and between 8 and 23 bars in the industrial *HPH*. The choice of a low range of operating pressure (compared to the usual range of pressure of several hundred bars in the case of milk homogenization) is motivated by the need of producing a metastable homogenized cream (i.e. that will not recoalesce after homogenization). The reservoir of amphiphilic components (such as caseins) being smaller in concentrated cream than in milk, the increase of interfacial area in cream is limited as compared to milk, hence explaining the use of a

lower range of pressure for concentrated cream homogenization. The cream is heated at 80°C prior to being processed. At the homogenizer outlet, the cream is cooled down to 20°C in a tubular heat exchanger and a sample is collected and stored at 4°C for granulometric analysis. Size distributions of cream fat globules obtained in these conditions are presented and discussed in the next section.

3. Results

3.1. Pilot *HPH*

Size distributions of fat globules at the outlet of the pilot *HPH* are displayed in Fig. 2 at different pressures. Fig. 2(a) shows the volume probability density function (*pdf*), noted $P(d)$ and 2(b) the corresponding cumulative probability distribution (*CPD*), noted $C_P(d)$. It can be observed that the *pdfs* are monomodal and are shifting towards smaller diameters as the operating pressure is increased, as a result of the breakup of the fat globules in the *HPH*. While the inlet diameter ranges between 0.8 and 8 μm, the outlet diameter at ΔP=60 bars ranges between 0.2 and 3.6 μm. Interestingly, when comparing the inlet to the outlet size distribution at a given pressure, they look self-similar, i.e. the outlet distribution can be deduced by dividing the diameters of the inlet distribution by a unique factor K, keeping constant the volume fraction. This self-similarity can be checked on the *CPDs*: for any given diameter of the inlet *CPD* (blue curve in Fig. 2(b)), the corresponding diameter of the outlet distribution at same value of the *CPD*, is obtained by drawing a horizontal line on the graph. One then can observe that the ratio between the inlet and outlet diameters is approximately constant for all diameters. This observation is verified at all pressures investigated.

This means that the outlet *CPD* matches the inlet one by multiplying the abscissa by a factor K. This matching is illustrated in Fig. 3(a) where all curves are collapsing with the inlet distribution curve with a pretty good level of approximation, with a factor K which is an increasing function of the operating pressure. Another way to illustrate the self-similarity property is to plot outlet-to-inlet *pdf* ratio, noted K_x ($=P_o(d_{ox})/P_i(d_{ix})$) as a function of the inlet-to-outlet diameter ratio (d_{ix}/d_{ox}) for few characteristic diameters along the size distribution. This graph is represented in Fig. 3(b) for d_{20} ($C_P(d_{20}) = 20\%$), d_{Max} (diameter class of maximum volume fraction) and d_{90} ($C_P(d_{90}) = 90\%$), indicated in Fig. 2(b). For all pressures investigated, the evolution is very close to the first bisector (y=x), validating the self-similarity property of all outlet size distributions. As a result, the outlet *pdf* $P_o(d)$, can be deduced from the

inlet *pdf* $P_i(d)$, applying mass conservation:

$$\begin{cases} P_o(d_o)\delta d_o = P_i(d)\delta d \\ \Rightarrow P_o(d_o) = K P_i(d) = K P_i(K d_o) \\ \Rightarrow P_o(d) = K P_i(K d) \end{cases} \quad (1)$$

in which the factor K is a growing function of the operating pressure ΔP. Equation (1) turns to consider that in average, each diameter class d of the inlet distribution will break into single size fragments of size d/K, as schematized in Fig.4. Under the action of a local shear $\dot{\gamma}$, a globule of diameter d is stretched into a filament of length L that eventually breaks into equal size fragments of diameter $d_o = d/K$ (their number being imposed by the volume conservation).

The *pdf* predicted by equation (1) has been plotted in Fig. 5 and compared to the experimental curves for each operating pressure investigated in the pilot *HPH*. For each curve, K has been taken equal to the ratio d_{iMax}/d_{oMax} from the corresponding experimental size distributions (cf Fig. 2(b)). The agreement between this model and the experimental data is remarkably good. This breakup model therefore describes the size distribution of 35% cream in the pilot *HPH* within a significant range of operating pressure, by making use of a single parameter K.

3.2. Industrial scale *HPH*

The *pdf* and *CPD* of cream fat globules diameters measured in the industrial *HPH* are reported in Fig. 6(a) and 6(b) respectively. The *pdfs* are bimodal in this case, with the presence of a secondary distribution of finer fat globules separated from a primary one, which tends to get closer and slightly overlap with the secondary distribution, as the pressure in the *HPH* is increased. As shown by Fig. 6(b), the cumulated volume fraction of this secondary distribution is less than 10%.

Due to the presence of a secondary distribution, even if of low volume fraction, the self-similarity property of the outlet distribution with the inlet one is no longer conserved. However, this property can be evaluated on the primary distributions obtained at different pressures, trying to find for each of them, a mutliplication factor of the abscissa that would make them collapse on a single curve, as for the size distributions obtained at the pilot scale *HPH*. The result is shown in Fig. 7(a) where the collapse of the *CPDs* is quite convincing. They all merge with the inlet distribution for $d \geq d_{iMax}$, where d_{iMax} is the diameter of maximum volume fraction of the inlet *pdf*, equal to 2.82 μm (cf. Fig. 6(b)). The corresponding multiplication factor K_1 of the absicssa has been reported as a function of the inlet-to-outlet maximum volume fraction diameter, d_{iMax}/d_{o1Max} for all cases in Fig. 7(b) (d_{o1Max} is the diameter at maximum volume fraction of the primary distribution of the outlet distribution, see Fig. 6(b)). Here again, the matching between

these two quantities is impressive, suggesting that each diameter class of the inlet distribution breaks into two classes of fragments of contrasted sizes, the larger being composed of single size fragments, proportional to the parent globule size. The smaller size class of fragments feeds the secondary distribution displayed in Fig. 6, and the maximum volume fraction diameter of the secondary distribution, noted d_{o2Max}, seems to be nearly constant in the whole pressure range (around 0.16 μm). The proportionality of the smaller fragment size to that of the parent globule can also be tested, taking the ratio d_{iMax}/d_{o2Max} as the proportionality factor. Doing so, each size class d of the inlet distribution will feed the outlet distribution with fragments of only two different sizes: d_{o1}=d/K_1 and d_{o2}=d/K_2, with $K_1 = d_{iMax}/d_{o1Max}$ and $K_2 = d_{iMax}/d_{o2Max}$. The corresponding breakup process is described in Fig. 8. Introducing the volume fraction Φ_2 of the smaller fragments d_{o2}, and using mass conservation, one finds:

$$\begin{cases} P_o(d_{o2})\delta d_{o2} = \Phi_2 P_i(d)\delta d \\ P_o(d_{o1})\delta d_{o1} = (1-\Phi_2) P_i(d)\delta d \\ d = K_1 d_{o1} = K_2 d_{o2} \end{cases} \Longrightarrow \begin{cases} P_o(d_{o2}) = K_2\Phi_2 P_i(K_2 d_{o2}) \\ P_o(d_{o1}) = K_1(1-\Phi_2) P_i(K_1 d_{o1}) \end{cases} \tag{2}$$

So the outlet size *pdf* $P_o(d)$ writes:

$$P_o(d) = K_2\Phi_2 P_i(K_2 d) + K_1(1-\Phi_2) P_i(K_1 d) \tag{3}$$

Note that equation (1) is the particular case of Φ_2=0 in equation (3).

Using equation (3), the outlet *pdf* $P_o(d)$ can then be deduced from the inlet size distribution $P_i(d)$. Corresponding results are displayed in Fig.9. The matching between experimental *pdfs* and modelled *pdfs* deduced from equation (3) is quite good, with a slight underestimation of the overlapping zone of the primary and secondary distribution, which represents no more than 2-3% in volume. As the pressure is increased from 8 to 23 bars, the proportionality factor K_1 corresponding to the largest fragment is increasing, in the same way as K for the pilot *HPH*, whereas K_2 remains constant ($K_2 \simeq 18$) and Φ_2 increases from 6.5 to 8.7%.

These results show that the homogenization of cream in *HPHs* at different scales can be described by a model (given by equation (3)) containing three independent parameters, K_1, K_2 and Φ_2. K_1 describes the largest fragments resulting from the fragmentation of an initial globule, whereas K_2 describes the secondary fragments of the same breakup event (see Fig. 8). When, the *HPH* operating pressure increases, K_1 is found to increase while K_2 remains almost constant. In the case of homogenization of 35% cream in the pilot *HPH*, the volume fraction of the smaller

fragments is negligible and the model reduces to a single parameter K.

3.3. Milk in pilot scale *HPH*

Finally, a test of milk homogenization has been performed in the pilot *HPH* at 80°C and 120 bars. The resulting size *pdf* and *CPD* are reported in Fig. 10(a) and (b), respectively. In this case, the *pdf* of the outlet size distribution is also bi-modal, but with a strong overlapping of the primary and secondary distributions between 0.5 and 1 μm. Assuming the same fragmentation mechanism as for the cream, we have used model (3) to construct the outlet size distribution, taking $K_1 = d_{iMax}/d_{o1Max} = 2.22$, $K_2 = d_{iMax}/d_{o2Max} = 10$ and Φ_2=0.36. As can be seen in Fig. 10, the match of the calculated distribution with the experimental curve is also quite correct in this case, suggesting that this fragmentation mechanism is more related to the milk fat globule properties than to the bulk flow properties. It is also interesting to note that the identified value of K_1 for milk homogenization in the pilot *HPH* at 120 bars is smaller than that of K for the cream in the same equipment at 45 bars. This result suggests a predominance of viscous stress contribution to the deformation of fat globules in the *HPH*. A physical interpretation of fat globule deformation and fragmentation in the *HPH* is discussed in the next section.

4. Derivation of a predictive model

It can be concluded from the preceding section that the homogenization of cream and milk in the *HPH* can be described by a simple fragmentation mechanism of each fat globule, independent of its size and valid in a wide range of operating pressure. In what follows, we propose a physical interpretation of this mechanism based on a simple model of fat globule deformation in a time-dependent flow field. **?** and **?** developped a numerical model describing the streching, breakup and mixing of viscous filaments, in 2D-chaotic viscous flows in which the leading forcing term is due to local elongational strain rate. Here, we consider that the fat globule continuously stretches with time under the action of a local shear rate in the *HPH* and ends to break into a single fragment size or two fragment sizes. The largest diameter of the produced fragments (d_o or d_{o1} resp. in equations (1) and (3)) is supposed to be equal to the thickness of the stretched globule at the *HPH* outlet. This allows us to relate the proportionality constant K in equation (1) (or K_1 in equation (3)) to a single hydrodynamic parameter, which is a non-dimensional shear stress. This parameter is then correlated to the operating pressure through a macroscopic scaling analysis of dissipation rate in the *HPH*. Therefore, the model presented below intends to provide a physical interpretation of the proportionality factor K (or K_1) in the breakup model.

4.1. Dynamic model of fat globule stretching

The model is a balance between the hydrodynamic forces exerted by the external flow on the fat globule, which tends to deform it, and the resistive forces that tend to oppose this deformation. A first important assumption is that for a fat globule of diameter d at 80°C, the resistance to the deformation is supposed to be controlled by the internal viscosity μ_d of the fat globule (mixture of triglycerides), the interfacial forces due to surface tension or viscoelastic modulus (**?**) being supposed negligible. This is the case because the Ohnesorge number of the globule is larger than one: $Oh = \mu_d/\sqrt{\rho_d \sigma d} > 1$, with ρ_d the fat globule density and σ the interfacial tension (**?**). Note that interfacial tension includes here the viscoelastic contributions originating from interface structure and composition (**?**). During deformation, the shape of the stretched globule is assumed to be a cylinder of radius $e(t)$ and length $L(t)$, as sketched in Fig. 4 and 8.

Then it is postulated that the external force per unit surface acting on the globule in the *HPH* is the viscous shear stress $\mu_e \dot{\gamma}(t)$, where μ_e is the effective viscosity of the external phase (35% cream) and $\dot{\gamma}(t)$ is the shear rate acting on the globule along its trajectory in the *HPH*. This viscous stress is assumed to result from the mean planar jet flow developing at the gap outlet in the ring chamber. This assumption will be discussed and validated in the next two sections. The resulting force balance along the globule trajectory through the *HPH* reads:

$$\mu_d \frac{1}{e}\frac{dL}{dt} = \mu_e \dot{\gamma}(t) \tag{4}$$

Making use of mass conservation ($6e^2 L = d^3$ (where d is the diameter of the native fat globule), equation (4) can be integrated over the residence time T_r of the fat globule in the *HPH*. The averaged radius of the filament e_o at the *HPH* outlet hence reads:

$$e_o \simeq \frac{d}{2}\left\{1 + \frac{1}{\lambda}\langle \int_0^{T_r} \dot{\gamma}(t)\,\mathrm{d}t \,\rangle\right\}^{-1/3} = \frac{d}{2}\left\{1 + \frac{1}{\lambda}\langle\dot{\gamma}\rangle T_r\right\}^{-1/3}, \tag{5}$$

in which the brackets denote the average over the residence time T_r and $\lambda = \mu_d/\mu_e$ is the viscosity ratio. Let K' be defined as:

$$K' = \left\{1 + \frac{1}{\lambda}\langle\dot{\gamma}\rangle T_r\right\}^{1/3} \tag{6}$$

The proposed model therefore predicts that the thickness $2e_o$ of the stretched globule at the *HPH* outlet is propor-

tional to its diameter:

$$2e_o = d/K' \tag{7}$$

In equation (7), the parameter K' embeds the effect of the flow hydrodynamics in the *HPH* on the fat globule deformation.

4.2. Breakup criterion and fragmentation model

Due to the Rayleigh Plateau instability, a fluid cylinder is unconditionally unstable (**?**). Thus, we assume that all fat globules passing through the HPH eventually breaks after having being stretched into a long filament. A simple fragmentation model consists in assuming that the filament will eventually break into fragments of equal size d_o or in two fragment sizes d_{o1} and d_{o2} as sketched in Fig.8, with d_o and d_{o1} being of the order of the filament thickness $2e_o$:

$$d_o \text{ or } d_{o1} \simeq 2e_o = d/K' \tag{8}$$

The physical reality of such a deterministic fragmentation process has been experimentally evidenced in the paper of **?** where images of aligned equal size fragments have been captured at the outlet of a model *HPH* device (flow in a duct through a planar restriction), resulting from the breakup of elongated filaments. It is important to mention that the experiments of **?** have been carried out with oil-in-water emulsions of high internal viscosity, corresponding to Ohnesorge numbers larger than 1. This fragmentation model predicts that each size class d_{ei} of the size distribution of the fat globules at the *HPH* entry, of probablity density $P_e(d_{ei})$, either feeds a single class of fragment d_{oi} or two classes of fragments d_{o1i} and d_{o2i}, the probability density of which is imposed by the mass conservation expressed in equations (1) or (2). Therefore, according to the proposed model, values of K and K_1, factors of respectively the single and two classes fragment breakup models (1) and (3), are equal to K'. Equation (6) therefore relates the breakup constants K (or equivalently K_1) to a single parameter, $\langle\dot{\gamma}\rangle T_r/\lambda$, which is a non-dimensional stress. It represents the averaged stress experienced by each fat globule along its trajectory in the *HPH*. The mean residence time T_r is the *HPH* volume divided by the volumetric flowrate, and $\langle\dot{\gamma}\rangle$ is the average shear rate exerted by the flow on each globule along its trajectory, which depends upon the *HPH* geometry and operating pressure ΔP. The larger $\langle\dot{\gamma}\rangle$, T_r and $1/\lambda$ (i.e., the larger μ_e), the larger K, and the smaller the outlet globule diameter (d_o or d_{o1}). If one admits that at constant T_r (or flowrate), $\langle\dot{\gamma}\rangle$ is a growing function of ΔP, then the present model is consistent with the observed trends of K with the operating pressure. Also, the former comparison of K_1 value for the milk at 120 bars with the K values for the cream

at much lower pressure, is consistent with the effect of the effective viscosity μ_e predicted by the model: for a given $\langle\dot{\gamma}\rangle$, the higher μ_e, the higher K. This result confirms the role of external phase viscosity in the breakup mechanism of fat globules in the *HPH*. The assumption of a viscous stress as the major cause of globule deformation can be justified here by the fact that any inertial contribution would be globule size-dependent and would result in a non-linear relation between the fragment size and the parent globule size. Note that this observation and the deterministic character of this fragmentation process makes unlikely a turbulence-induced breakup mechanism (inertial or viscous). The next section is devoted to the establishment of the relation between $\langle\dot{\gamma}\rangle$ and ΔP.

4.3. Modeling of the relation between K and ΔP

As presented in section 2.3, the emulsion in the *HPH* experiences a radial flow in a cylindrical gap of few tens of micrometers thickness, connecting the impact ring chamber (see Fig.1). The deformation of the globule being supposed to be due to the viscous shear stress exerted by the mean jet flow in the impact ring chamber, the averaged shear rate $\langle\dot{\gamma}\rangle$ can then be estimated according to:

$$\langle\dot{\gamma}\rangle \propto \frac{U_\delta}{\delta/2} \tag{9}$$

Due to mass conservation in a cylindrical channel section, U_δ is inversely proportional to δ. Hence equation (9) leads to:

$$\langle\dot{\gamma}\rangle \propto \Delta P_R \tag{10}$$

Next step is to determine the relation between ΔP_R and the total pressure difference in the *HPH*, Δ_P. ΔP is supposed to be the sum of two main contributions, the pressure drop in the gap radial flow of thickness δ, noted ΔP_δ, and the pressure drop due to the discharge in the impact ring chamber, ΔP_R:

$$\Delta P \simeq \Delta P_\delta + \Delta P_R \tag{11}$$

The Reynolds number in the gap being independent of the gap thickness, it is straightforward to show that the pressure drop in the gap ΔP_δ is proportional to δ^{-3}, whether the flow in the gap is laminar or turbulent (see Appendix A). The pressure drop ΔP_R is assumed to be proportional to U_δ^2, as in a sudden expansion flow, where U_δ is the mean velocity

in the gap. Due to mass conservation in a cylindrical channel section, U_δ is inversely proportional to δ. Hence, ΔP_R varies as δ^{-2} and ΔP_δ is proportional to $\Delta P_R^{3/2}$. Equation (11) can then be written as:

$$\Delta P = \alpha \Delta P_R^{3/2} + \Delta P_R \tag{12}$$

The calculation of ΔP_δ and α in both laminar and turbulent regimes is developped in Appendix A. In all cases, it is possible with equation (12) to relate for a given fluid system and at a given flowrate, ΔP_R to the operating pressure ΔP in the *HPH*. For the 35% cream at 80°C, the gap flow in the pilot *HPH* is found to be laminar, whereas it is turbulent in the industrial *HPH*. In both cases, the evolution of ΔP_R with ΔP provided by equation (12), can be very well represented by a power law ($\Delta P_R = a \Delta P^b$), with the prefactor a and the exponent b close to 1. Hence, in the range of operating pressure ΔP investigated, the discharge pressure drop ΔP_R can be fairly identified to the pressure drop in the *HPH* ($\Delta P_R \simeq \Delta P$).

From equations (10), the proportionality factor K' given by equation (6) can be expressed as a function of ΔP according to:

$$K' = \left\{1 + k' \Delta P\right\}^{1/3} \tag{13}$$

where k' is a parameter which depends upon *HPH* geometry and flow properties. This model has been tested in Fig.11(a) against the experimental values of K and K_1 obtained with the 35% cream at 80°C, respectively in the pilot (closed blue rounds) and industrial (closed red rounds) *HPH*. The data can be reasonably well described by the following model:

$$K' = 0.6 \left\{1 + 1.2 \Delta P\right\}^{1/3} \tag{14}$$

This result first shows that the fragmentation model proposed leads to a suitable model of the fragmentation constants K and K_1 as a function of ΔP. The value of the prefactor is found to be smaller than 1 (0.6), probably because in the low range of K values, the approximation of the stretched globule as a cylinder is not accurate (an overestimation of 22% is observed for the lowest pressure in the pilot *HPH*). It also validates the scaling of $\langle \dot{\gamma} \rangle$ given by (10).

4.4. Prediction of K' from numerical simulations

To complete this study, the parameter K' given by equation (6) has been estimated from numerical simulations of single-phase flow in the two *HPHs* geometries investigated in this study. The objective was to compute the average quantities $\langle\dot{\gamma}\rangle$ and T_r (residence time of the particle in the calculation domain) seen by a fat globule along its trajectory. In these simulations, the cream was considered as a homogeneous Newtonian fluid, and flowrates were set identical to those of the experiments (Q=200 and 8800 L/h for the pilot and industrial *HPH*, respectively). The numerical method, the calculation domain and typical flow structure are described in appendix B. One test case was performed at a pressure of 100 bars in the pilot *HPH* and three test cases in the industrial *HPH*, at 40, 70 and 115 bars, were done. In each case, several thousands of fluid particles of the emulsion, which is treated as a homogeneous fluid, initially homogeneously distributed in the gap flow entry, were individually tracked in the impact ring chamber, and K' was obtained by averaging the shear rate experienced by all fluid particles along their trajectory. For each particle, $\langle\dot{\gamma}\rangle = \langle\sqrt{2D:D}\rangle$ (where D is the local deformation rate tensor), T_r is directly computed and K' is derived from equation (6). For all these simulations, the flow viscosity μ_e was arbitrarily set to 1.16×10^{-3} Pa.s, which corresponds to $\lambda=\mu_d/\mu_e$=9.25 (this bulk viscosity corresponds to a laminar regime of the gap flow in the pilot *HPH*, close to the transition, and to a turbulent gap flow in the industrial *HPH*). The resulting *CPD* $F(K')$ is displayed in Fig.11(b) for all test cases. It exhibits a multimodal shape with a principal mode corresponding to more than 50% of the distribution. The averaged value is indicated by a round symbol on each curve.

These averaged values of K' are reported in Fig.11(a) for both pilot and industrial *HPHs*, represented by open symbols. Their order of magnitude is close to the values of K and K_1 obtained for the cream, respectively in the pilot and industrial *HPH*, but they tend to deviate from the trend observed for the cream, with smaller values as those predicted by the model (equation (14)). In Fig.11(a), the experimental value obtained for K_1 in the case of milk at 120 bars in the pilot *HPH* has been also reported and its value is also widely below the trend observed for cream. These results confirm that the bulk viscosity favors the breakup efficiency and increase the value of K or K_1. In order to account for the effect of viscosity, a correction under the form of a power law of the viscosity ratio λ^{-b} has been introduced in equation (14). Taking b=0.4, this correction seem to regroup the data on a single curve, as shown in Fig.12, with an average discrepancy of 8.5%.

These results give support to the present model for the viscous deformation mechanism and break-up of the fat globules in the *HPHs*, and confirm the relevance of the hydrodynamic parameter $\langle\dot{\gamma}\rangle T_r/\lambda$ to quantify homogenization efficiency of dairy cream. They also confirm the scaling proposed for its relation with the operating pressure ΔP, at both pilot and industrial scales.

It must be stressed that this simple micro-scale model of the stretching of a non-relaxing viscous cylindrical fila-

ment does not claim to describe exactly the flow in a *HPH*, but it intends to account for the main physical mechanisms in order to understand the characteristics of the shape distributions generated in HPHs. There are two underlying reasons to the success of this model. First, the fat globule resistance to deformation is controled by the internal viscosity and not by the surface stress, so its relaxation time is always much larger than the characteristic time of shearing in a *HPH*. In the particular case of dairy cream, this is characterized by a value of the Ohnesorge number larger than unity. The second reason is the *HPH* flow geometry, which forces the each fat globule to undergo the same range of deformation within a given residence time (like in a Couette apparatus), so the description of the forcing term at the scale of an individual globule by a single hydrodynamic scale - the averaged shear rate - is relevant for the whole emulsion. We therefore believe this model builds up a valuable tool for the dairy industry engineers, regarding the understanding of dairy cream homogenization and the optimization of *HPH* parameters.

4.5. Secondary distribution

The fragmentation model of fat globules in *HPHs* considers two contrasted fragment sizes (cf. equation (3)), both being proportional to their parent fat globule size. The larger fragment size has been related to the operating pressure, the smaller one seems to be quasi-constant and independent of ΔP, at least in the range of operating pressure in the industrial *HPH* (between 8 and 23 bars). This breakup mechanism hence involves two more parameters that needs to be modeled: the size reduction constant K_2 and the volume fraction Φ_2 (or the number of fragments). The formation of satellite drops during the fragmentation of a viscous filament is well documented in the literature (**?**). Satellite drops results from the breakage of the thin bridge developing between two separating main bulbs in the latter stage of the fragmentation process. The production of satellite drops could depend on the local hydrodynamics in the HPH (Reynolds number and turbulence level), but we have no means to propose a predictive model for these satellite drops at the moment. The prediction of their size and volume fraction requires a detailed and complex analysis involving surface stress properties, which is beyond the scope of the present paper. However, the fact that the size of the secondary fragments are found to be proportional to that of parent fat globule is in qualitative agreement with the present deformation model, since for given shear rate and residence time, a smaller drop is stretched in a thinner filament than a larger drop, leading to a thinner bridge eventually separating fragments and to the formation of smaller satellite drops. Also, the increasing volume fraction of the satellite drops as the operating pressure is increased, is consistent with the fact that the larger the fat globule extension, the longer the developing thin film, and the larger the number of satellite drops.

5. Conclusion

Homogenization of 35% dairy cream at pilot and industrial scales was investigated in this work. The analysis of fat globules size distributions at the pilot *HPH* outlet operated at different pressures shows that they are self-similar to the inlet size distribution. This means that the size distribution of the homogenized cream can be deduced by considering a single fragment size for each fat globule entering the *HPH* with the same volume (or mass) fraction. Size distributions measured at the outlet of the industrial *HPH* were found to be bimodal with two characteristic distributions centered around a large and a small fragment sizes with a small overlapping. In this case, the two distributions can be also reconstructed from the inlet distribution by considering only two fragment sizes issued from each individual inlet globule. In both cases, the size of the largest fragment produced is proportional to the inlet fat globule diameter, and the proportionality factor is independent of the inlet globule size. This simple model was also successfull at predicting the size distribution of fat globules issued from milk homogenization in the pilot *HPH*. The physics of this fragmentation mechanism was then interpreted by considering the dynamics of the deformation of a fat globule into a cylindrical filament, resulting from the balance between the external time dependent viscous stress and the internal viscous stress of the stretched globule. Then it was assumed that the breakup of this filament at the *HPH* outlet leads to the formation of a single- or two-fragment size population, with the largest fragment size scaling as the filament thickness. From that theoretical framework, the self-similarity factor deduced from the experiments could be related to a single hydrodynamic parameter, a non-dimensional stress which was modeled as a function of the operating pressure of the *HPH*. The evaluation of this scaling law with experimental values of the proportionality factor obtained at both *HPH* scales showed a good agreement, also validated by numerical simulations performed in real *HPH* geometries. This elementary fragmentation mechanism of fat globules is thought to result from two specific conditions: first the relaxation time of the fat globule shape is much larger than any flow time scale in the *HPH*, so breakup always occurs at maximum stretching of the globule. This property is due to the high internal viscosity of the fat globule, which overcomes any viscoelastic property of the interface. The second condition is due to the flow configuration generated in a *HPH*, where the whole emulsion is submitted to the same level of shear rate. It results that all fat globules flowing through the thin gap of the *HPH* experience the same average shear rate, so the hydrodynamic stress can be reduced to a single parameter. The theoretical interpretation of this fragmentation mechanism of fat globules in *HPHs*, even though not an exact representation of the reality, is therefore believed to constitute a relevant guide for the optimization of process parameters and scaling up of dairy cream homogenization.

Credit author statement

The contributions of each of the authors were essential to the completion of this study, which is the result of a complex fruitful human collaboration.

A. Pressure drop contributions in the HPH

A.1. Pressure drop in the gap channel

The pressure drop in the gap channel, of length L_g and thickness δ can be estimated considering that the flow is established in the gap and that the flow section is constant between the entry and the outlet of the gap. The latter assumption is justified by the condition $L_g/R_0 << 1$ which is verified in both *HPH* geometries, where R_0 is the radius of the cylindrical gap (cf values of R_0 and L_g in table 1). The pressure drop in the gap can be expressed through the momentum balance integrated in the gap flow section:

$$\frac{\Delta P_\delta}{L_g} = \tau_w \frac{2}{\delta} \tag{15}$$

where τ_w is the wall shear stress in the gap. The velocity in the gag, U_δ, is equal to the flowrate, Q, divided by the gap crosssection:

$$U_\delta = \frac{Q}{2\pi R_0 \delta} \tag{16}$$

The Reynolds number in the gap, Re_δ is equal to:

$$Re_\delta = \frac{\rho_e U_\delta \delta}{\mu_e} = \frac{\rho_e Q}{2\pi R_0 \mu_e} \tag{17}$$

where ρ_e and μ_e are the cream density and viscosity respectively. Therefore, the Reynolds number is independent of the gap thickness. If the flow in the gap channel is laminar, the wall shear stress τ_w can be calculated assuming a steady established parabolic velocity profile, and taking its derivative at the wall:

$$\tau_w = 6\mu_e \frac{U_\delta}{\delta} \tag{18}$$

In laminar regime, the pressure drop in the gap reads:

$$\Delta P_\delta = 12\mu_e L_g \frac{U_\delta}{\delta^2} \tag{19}$$

Inserting (16) in (19) leads to:

$$\Delta P_\delta = \frac{12\mu_e L_g Q}{2\pi R_0 \delta^3} \tag{20}$$

For a given flowrate in a given geometry, the pressure drop in the gap varies as δ^{-3} in laminar regime. If the flow in the gap channel is turbulent and established, the wall shear stress can be expressed as a function of the friction velocity at the wall, u^*, which is related to the mean velocity in the gap, U_δ through the friction factor $f(Re_\delta)$:

$$\tau_w = \rho_e u^{*2} = \rho_e f \frac{U_\delta^2}{2} \tag{21}$$

The pressure drop in the gap hence reads in turbulent regime:

$$\Delta P_\delta = \frac{12\rho_e f L_g Q^2}{4\pi^2 R_0^2 \delta^3} \tag{22}$$

As f is a function of gap Reynolds number Re_δ which is independent of gap thickness δ, in turbulent regime, the pressure drop in the gap is also proportionnal to δ^{-3}. Taking ρ_e=958 kg/m^3 and μ_e=2.89×10^{-3} for the 35% w/w cream at 80°C, Re_δ can be calculated in both *HPH* geometries. In the pilot *HPH*, at a flowrate $Q = 200L/h$, Re_δ=730, and in the industrial *HPH*, Re_δ=3200 for a flowrate $Q = 8800L/h$. Hence, the flow is laminar in the pilot *HPH* and turbulent in the larger scale *HPH*. With milk at 80°C and $Q = 200L/h$ in the pilot *HPH*, Re_δ=3500, so the flow in the gap channel is turbulent.

A.2. Pressure drop in the impact ring chamber

The pressure drop in the impact ring chamber, ΔP_R can be approximated by:

$$\Delta P_R \sim \rho_e \frac{U_\delta^2}{2} \tag{23}$$

As a result, for both laminar and turbulent regimes in the gap flow, ΔP_δ scales as $\Delta P_R^{3/2}$:

$$\Delta P_\delta = \alpha \Delta P_R^{3/2} \tag{24}$$

Making use of equations (20) and (22), the factor α in equation (24) can be determined in laminar and turbulent regime:

1. Laminar regime

$$\alpha = \frac{48\mu_e L_g(\pi R_0)^2}{Q^2}(\frac{2}{\rho_e})^{3/2} \tag{25}$$

2. Turbulent regime

$$\alpha = \frac{32\rho_e f L_g \pi R_0}{Q}(\frac{2}{\rho_e})^{3/2} \tag{26}$$

with:

$$f = 0.073 Re_\delta^{-1/4} \tag{27}$$

The total pressure drop in *HPH* is the sum of ΔP_R and ΔP_δ:

$$\Delta P = \Delta P_\delta + \Delta P_R = \alpha \Delta P_R^{3/2} + \Delta P_R \tag{28}$$

From relations (25) or (26), α can be computed in both *HPH* geometries. At a given operating pressure ΔP, ΔP_R can then be determined using (28). In all range of α values, equation (28) can be replaced by a simple power law $\Delta P_R = a\Delta P^b$, with a and b close to 1, as shown in Fig. 13. As a result, in the range of pressure investigated, the discharge pressure drop is identical to the pressure drop in the *HPH*. The values of gap Reynolds number, parameters α (in equation(28)), a and b are reported in table 2 for the cream in both *HPHs*, and in table 3 for milk in the pilot *HPH*.

B. Flow simulations in the *HPHs*

Computations were run using ANANAS^{TM} which solves the incompressible balance equations for mass and momentum. ANANAS^{TM} uses tetrahedral elements and is based on a mixed finite volume/finite element method. The domain geometry and the mesh grid used for the flow computation in the industrial *HPH* are shown in Fig. 14. Time integration is carried out using a third order explicit scheme, while space integration is handled with a high-order scheme introduced by **?**, which yields to a sixth-order accuracy for an uniform mesh spacing. Depending on the case and Reynolds number value, the turbulence can be either modelled with a *k-ε RANS* model as proposed by **?** or thanks to Large Eddy Simulation Variational Multi-Scale model (*LES-VMS*) which enables the resolution of turbulent structures scaling down to the mesh size (**?**). Contrarily to common *LES* approaches, *LES-VMS* reduces spurious

dissipation. Simulations of pilot and industrial *HPHs* have been achieved with different numerical models. At pilot scale, a transitional problem occurs in the jet while a fully turbulent flow is identified at industrial scale. It is why all the simulations have been run using *LES-VMS* at the pilot scale and a k-ϵ model was chosen for the simulation of the industrial *HPH*.

In these simulations, the density of the fluid is ρ_e=958 kg/m^3 and the viscosity is μ_e=1.16×10^{-3} Pa.s. The operating pressure, gap (average) thickness and gap average velocity are reported in table 4 for the pilot and industrial *HPH*. Gap Reynolds numbers (equation (17)) are respectively 1800 and 8000 for the pilot and industrial *HPH*.

In Figs.15 and 16, typical velocity fields respectively obtained in the pilot and industrial scale *HPHs* are displayed. The regions of highest shear are generated around the jet, in the impact ring wall region, and in the recirculation loops developing in the whole chamber.

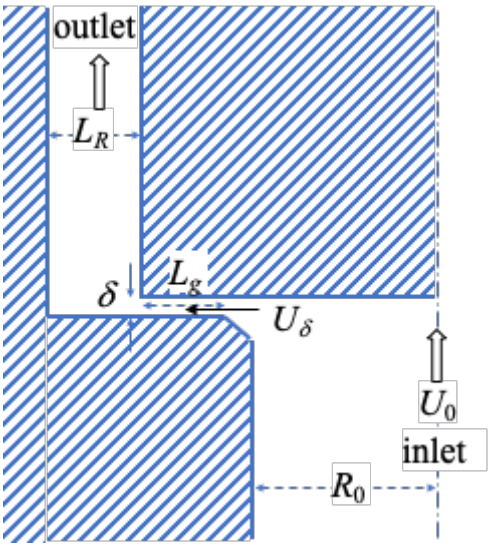

Figure 1: Schematic of the *HPH*. δ=$O(10-10^2\mu m)$ is the gap thickness, U_0 is the inlet velocity of the emulsion and $L_R = O(10^2 \times \delta)$ is the width of the impact ring chamber.

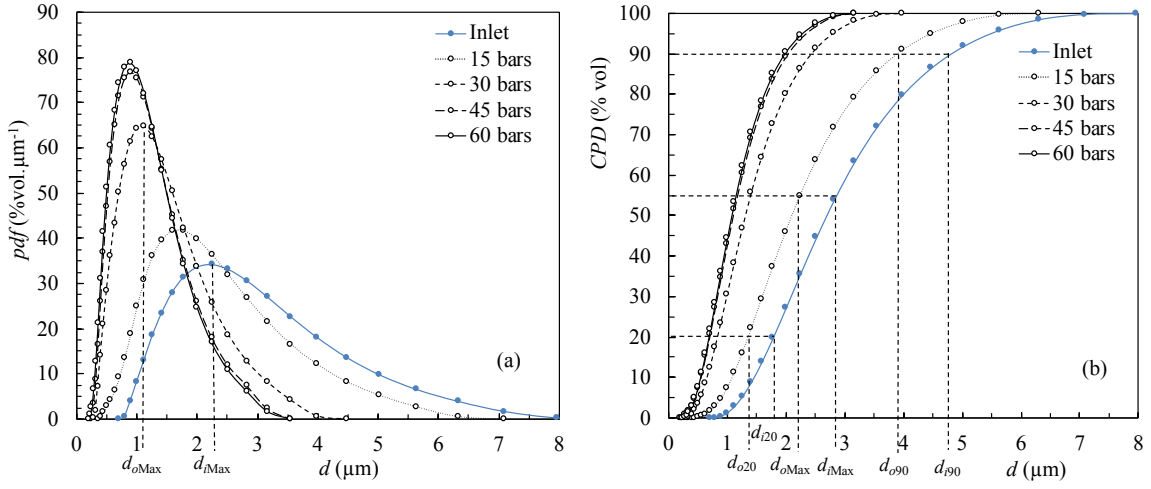

Figure 2: Experimental size distribution in the *pilot scale HPH* at different pressures. (a) Probability density function (*pdf*) ; (b) Cumulative probability distribution (*CPD*). Characteristic diameters ($d_{i20}, d_{iMax}, d_{i90}$) and ($d_{o20}, d_{oMax}, d_{o90}$) correspond to the inlet and outlet distributions at 15 bars, respectively.

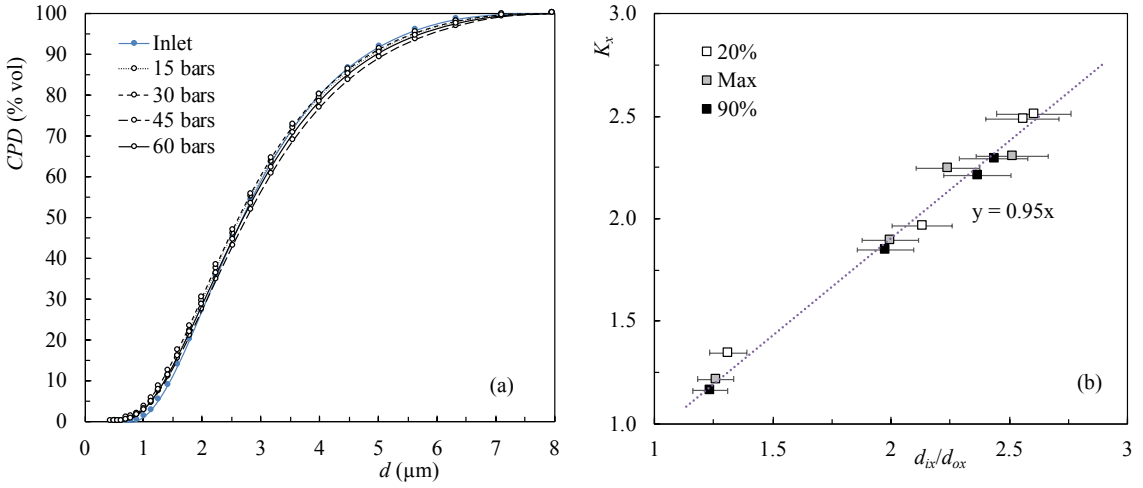

Figure 3: (a) Same curves as in Fig. 2(b) for the pilot *HPH* after multiplying the abscissas by a factor K (K = 1.27, 2, 2.35 and 2.51) respectively for (ΔP=15, 30, 45 and 60 bars). (b) Outlet-to-inlet *pdf* ratio $K_x = P_o(d_{ix})/P_o(d_{ox})$ at three different characteristic diameters d_x as a function of inlet-to-outlet diameter ratio (d_{ix}/d_{ox}) for all operating pressures investigated. The characteristic diameters are d_{20}, d_{Max} (diameter of maximum volume fraction of the distribution), and d_{90}. Error bars correspond to the width of a size class divided by the class size (i.e. ±6%). The uncertainty on K_x is smaller than the symbol size on this graph.

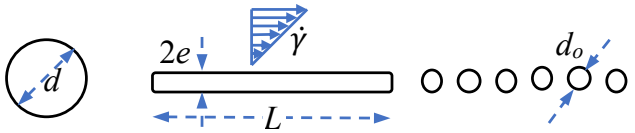

Figure 4: Scheme of fat globule breakup in the pilot *HPH*

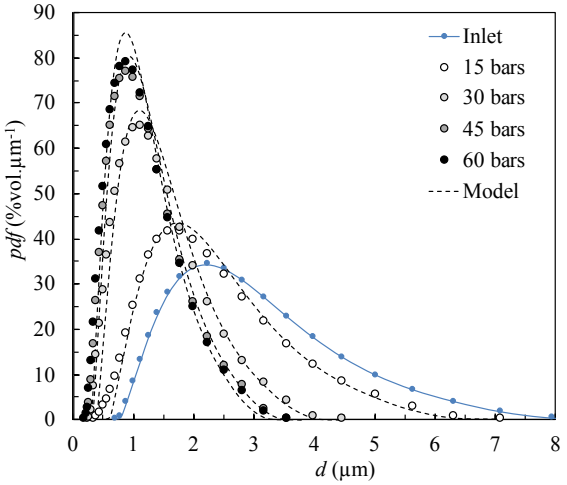

Figure 5: *pdfs* of cream globule size in the *pilot HPH*. Comparison between model (dashed line) and experiments (symbols) (K = 1.27, 2, 2.35 and 2.51) respectively for (ΔP=15, 30, 45 and 60 bars)

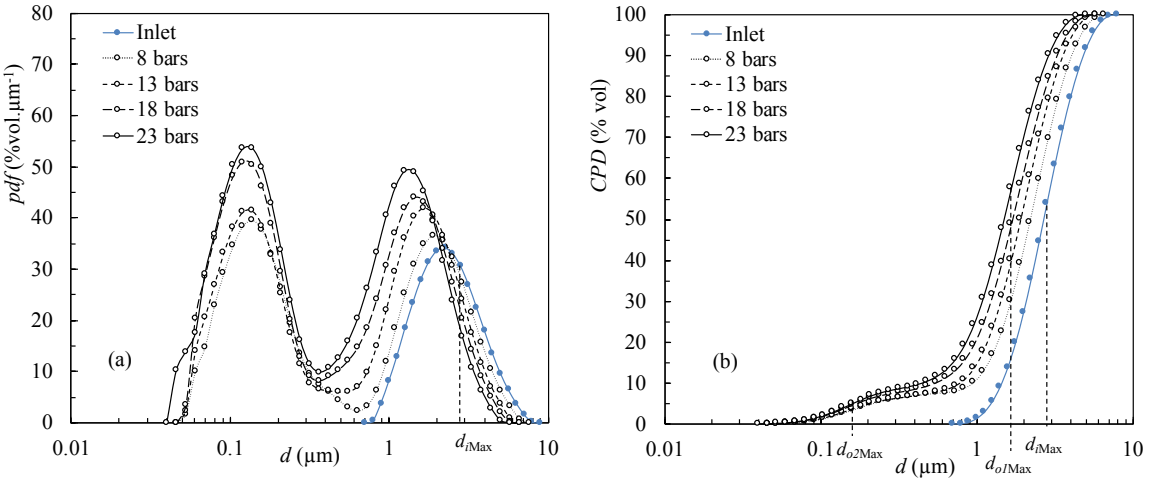

Figure 6: Experimental size distribution in the *industrial HPH* at different pressures. (a) *pdf* ; (b) *CPD*.

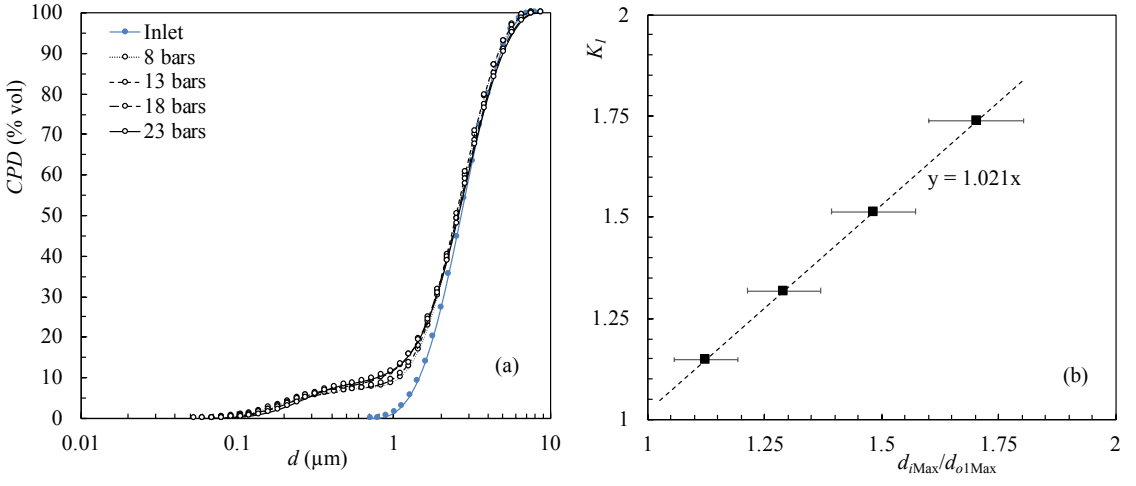

Figure 7: (a) Same curves as in Fig.6(b) for industrial *HPH* after multiplying the abscissas by a factor K_1 (K_1 = 1.12, 1.29, 1.48 and 1.70) for (ΔP= 8, 13, 18 and 23 bars), respectively. (b) K_1 as a function of inlet-to-outlet maximum volume fraction diameter ratio. Error bars correspond to the width of a size class divided by the class size (i.e. ±6%). The uncertainty on K_1 is smaller than the symbol size on this graph.

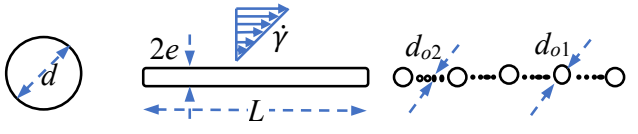

Figure 8: Scheme of fat globule break-up in the industrial scale *HPH*

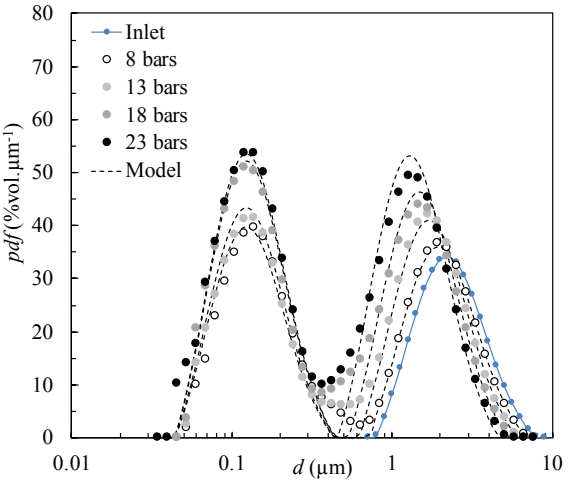

Figure 9: *pdfs* of cream globule size in the *industrial scale HPH*. Comparison between model (dashed line) and experiments (symbols) K_1=(1.12, 1.29, 1.48 and 1.70) and Φ_2=(6.5, 7.1, 8.6 and 8.7 %) respectively for ΔP=(8, 13, 18 and 23 bars). K_2=17.8 for all cases

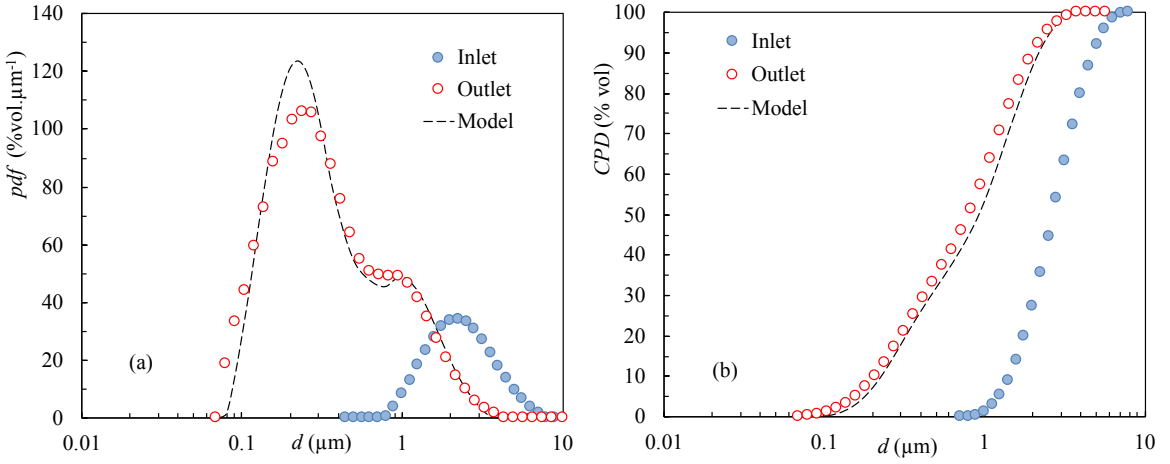

Figure 10: Size distribution of milk fat globules in the pilot scale *HPH* at 120 bars and 80°C. Comparison between model (dashed line) and experiments (symbols). (a) *pdf* (b) *CPD* (K_1=2.22, K_2=10, Φ_2 = 36%)

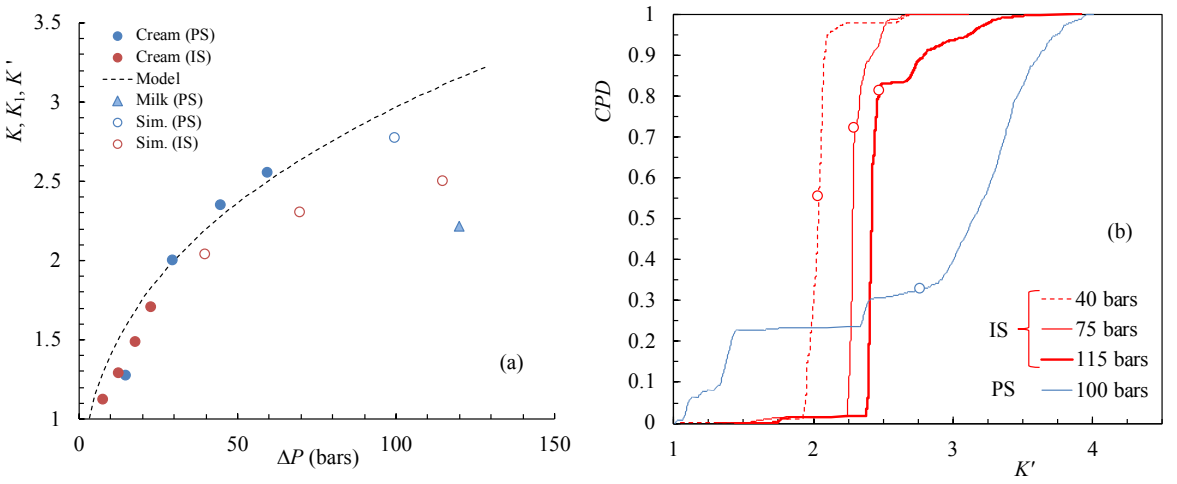

Figure 11: (a) Evolutions of K, K_1 and K' as a function of ΔP in the *HPHs*. Blue symbols: pilot scale. Red symbols: industrial scale. Open symbols are obtained from numerical simulations. The triangle symbols shows the case of milk (ρ_e=1000 and μ_e=0.64×10^{-3} at 80°C) at 120 bars in the pilot *HPH* (b) *CPD* of K' from numerical simulations. $K'=(1+\langle\dot{\gamma}\rangle T_r/\lambda)^{1/3}$, with λ=9.25 (μ_e=1.16×10^{-3}). On each curve, the round symbol represents the average value. Blue color: pilot scale (PS), with K'=2.77 for ΔP=100 bars. Red color: industrial scale (IS) with K'=2.04, 2.30 and 2.50 for ΔP=40, 75 and 115 bars, respectively.

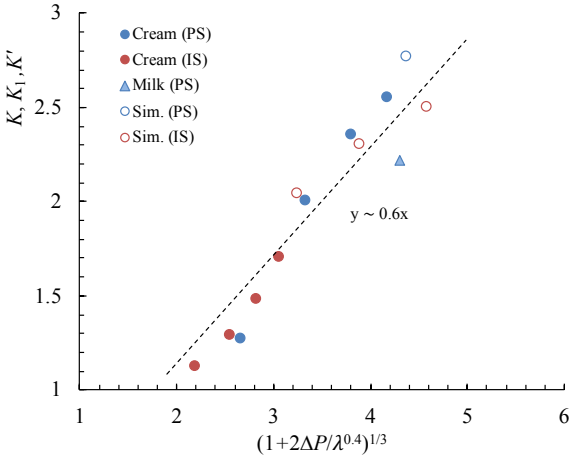

Figure 12: Fragmentation constant as a function of $(1+2\Delta P/\lambda^{0.4})^{1/3}$ for all systems in both *HPH* geometries. Closed round symbols: experimental data for cream λ=3.69 (μ_e=2.9×10^{-3}). Open round symbols: simulation data with λ=9.25 (μ_e=1.16×10^{-3}).Triangle symbol: milk with λ=1.69 (μ_e=0.63×10^{-3}). Blue color: pilot scale (PS). Red color: industrial scale (IS)

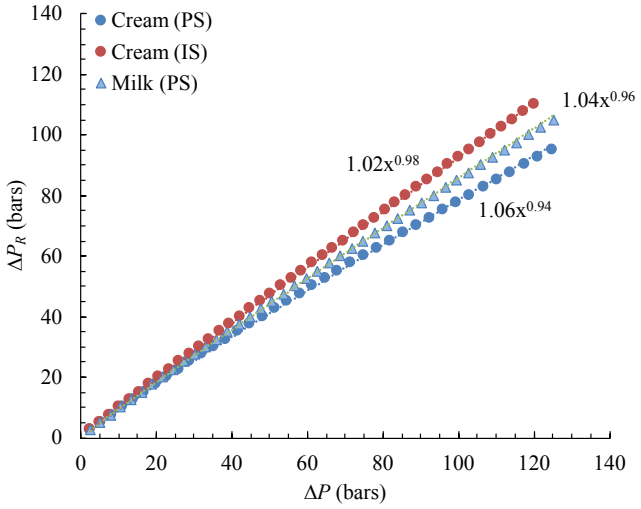

Figure 13: Discharge pressure drop in the ring chamber as a function of the *HPH* pressure for 35% concentrated cream at 80°C (ρ_e=960 kg/m^3 and μ_e=2.9×10^{-3}. Blue color: pilot scale (PS). Red color: industrial scale (IS)

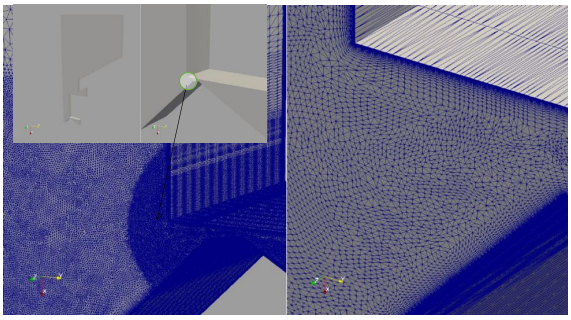

Figure 14: left: Domain geometry and unstructured mesh grid in the industrial *HPH*. right: zoom of the mesh grid in the gap outlet region.

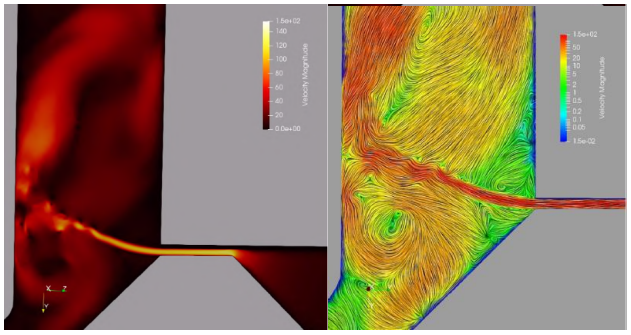

Figure 15: left: Snapshot of velocity magnitude field in the pilot *HPH* obtained from *LES* simulation. right: corresponding streamlines.

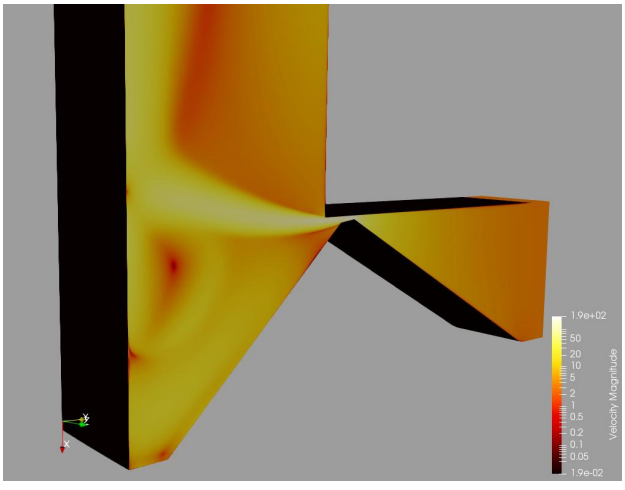

Figure 16: Velocity magnitude field in the industrial scale *HPH* obtained from *RANS* simulation.

	R_0 (mm)	L_g (μm)
Pilot	4	150
Industrial	40	300

Table 1
Inlet section radius and gap length of pilot and industrial *HPHs*.

μ_e=2.9×10^{-3}Pa.s	Q (L/h)	Re_δ	α (10^{-2}bars$^{-1/2}$)	a	b
Pilot	200	730	3.22	1.06	0.94
Industrial	8800	3200	0.964	1.02	0.98

Table 2
Flow rate, gap flow Reynolds number, parameter α in equation (28), parameters a and b in relation $\Delta P_R = a\Delta P^b$ for cream in pilot and industrial *HPHs*.

μ_e=0.63×10^{-3}Pa.s	Q (L/h)	Re_δ	α (10^{-2}bars$^{-1/2}$)	a	b
Pilot	200	3500	1.86	1.04	0.96

Table 3
Flow rate, gap flow Reynolds number, parameter α in equation (28), parameters a and b in relation $\Delta P_R = a\Delta P^b$ for milk in pilot *HPH*.

	$\Delta P(bars)$	δ (μm)	U_δ (m/s)
Pilot	100	17	129
Industrial	40	111	88
	70	82	118
	115	67	144

Table 4
Pressure, gap average thickness and velocity for the simulated cases